

# Ion Dynamics in Concentrated Electrolyte Solutions: Relating Equilibrium Fluctuations of the Ions to Transport Properties in Battery Cells

Bernhard Roling\* , Vanessa Miß, and Janosch Kettner

In recent years, the interest in the development of highly concentrated electrolyte solutions for battery applications has increased enormously. Such electrolyte solutions are typically characterized by a low flammability, a high thermal and electrochemical stability and by the formation of a stable solid electrolyte interphase (SEI) in contact to electrode materials. However, the classification of concentrated electrolyte solutions in terms of the classical scheme “strong” or “weak” has been controversially discussed in the literature. In this paper, a comprehensive theoretical framework is presented for a more general classification, which is based on a comparison of charge transport and mass transport. By combining the Onsager transport formalism with linear response theory, center-of-mass fluctuations and collective translational dipole fluctuations of the ions in equilibrium are related to transport properties in a lithium-ion battery cell, namely mass transport, charge transport and  $\text{Li}^+$  transport under anion-blocking conditions. The relevance of the classification approach is substantiated by showing that i) it is straightforward to classify highly concentrated electrolytes and that ii) both fast charge transport and fast mass transport are indispensable for achieving fast  $\text{Li}^+$  transport under anion-blocking conditions.

## 1. Introduction

State-of-the-art lithium-ion batteries employ typically 1 M electrolyte solutions, since the ionic conductivity becomes maximal in this concentration regime. However, in recent years, the interest in developing highly concentrated electrolyte solutions for battery applications has increased enormously. Examples encompass highly concentrated carbonate-based solutions,<sup>[1–7]</sup> highly concentrated sulfolane-based electrolytes,<sup>[8–11]</sup> solvate ionic liquids,<sup>[12,13]</sup> water-in-salt electrolytes<sup>[14–16]</sup> and localized high-concentration electrolytes.<sup>[6,17–19]</sup>

These electrolyte solutions are being developed for several reasons:


i) In highly concentrated solutions, a major part of the solvent molecules is involved in the solvation of the ions, so that only few “free” solvent molecules exist. This leads to a low chemical potential and low

vapor pressure of the solvent molecules and thus to a low flammability of the electrolyte. ii) The low chemical potential of the solvent molecules improves the electrochemical and thermal stability of the electrolyte solution. iii) A strong binding of solvent molecules to the  $\text{Li}^+$  ions leads to the formation of a so-called “anion-derived” solid electrolyte interphase (SEI) at the negative electrode of a lithium-ion battery, which is mainly composed of anion decomposition product.<sup>[20,21]</sup> Such anion-derived SEIs have been shown to exhibit a high long-term stability. iv) It has been observed that highly concentrated electrolytes suppress the formation of Li dendrites in Li metal batteries.<sup>[2,5]</sup>

These advantages of highly concentrated electrolytes for battery applications are often counterbalanced by slower charge and mass transport as compared to 1 M solutions. Therefore, it is important to obtain an improved understanding of transport processes in concentrated electrolyte solutions and to optimize their transport properties. Although a number of transport models for concentrated electrolyte solutions has been developed,<sup>[22–26]</sup> their classification in terms of the classical scheme “strong” or “weak” has been controversially discussed in the literature.<sup>[27–32]</sup>

In a recent Frontier Outlook,<sup>[33]</sup> we have suggested a more general classification, which is based on a comparison of charge and mass transport in the electrolyte. To this end, we defined a molar mass transport coefficient  $\Lambda_{\text{mass}}$ , which is the mass transport analogue of the molar ionic conductivity  $\Lambda_{\text{charge}}$  and which, according to linear response theory, is related to center-of-mass fluctuations of the ions in thermal equilibrium.<sup>[33]</sup> Based on this, we distinguished “weak charge transport electrolytes” with  $\Lambda_{\text{charge}} \ll \Lambda_{\text{mass}}$  from “weak mass transport electrolytes” with  $\Lambda_{\text{mass}} \ll \Lambda_{\text{charge}}$ . In “weak charge transport electrolytes,” the strong interactions between cations and anion as compared to ion/solvent interactions leads to charge transport limitations, see **Figure 1a**. An example in the field of  $\text{Li}^+$  electrolyte solutions are strong interactions between  $\text{Li}^+$  ions and trifluoroacetate anions, see **Figure 1b**. In contrast, in “weak mass transport electrolytes,” the strong interactions between cations and solvent molecules as compared to cation/anion interactions reduces the momentum exchange between ions and solvent molecules and thus the center-of-mass fluctuations of the ions and the mass transport, see **Figure 1a**. An example are the strong interactions between  $\text{Li}^+$  ions and triglyme molecules (G3) in solvate ionic liquids containing

Prof. Dr. B. Roling, Dr. V. Miß, J. Kettner  
Department of Chemistry, University of Marburg, Hans-Meerwein-Str. 4,  
35032 Marburg, Germany  
E-mail: roling@staff.uni-marburg.de

 The ORCID identification number(s) for the author(s) of this article can be found under <https://doi.org/10.1002/eem2.12533>.

DOI: 10.1002/eem2.12533

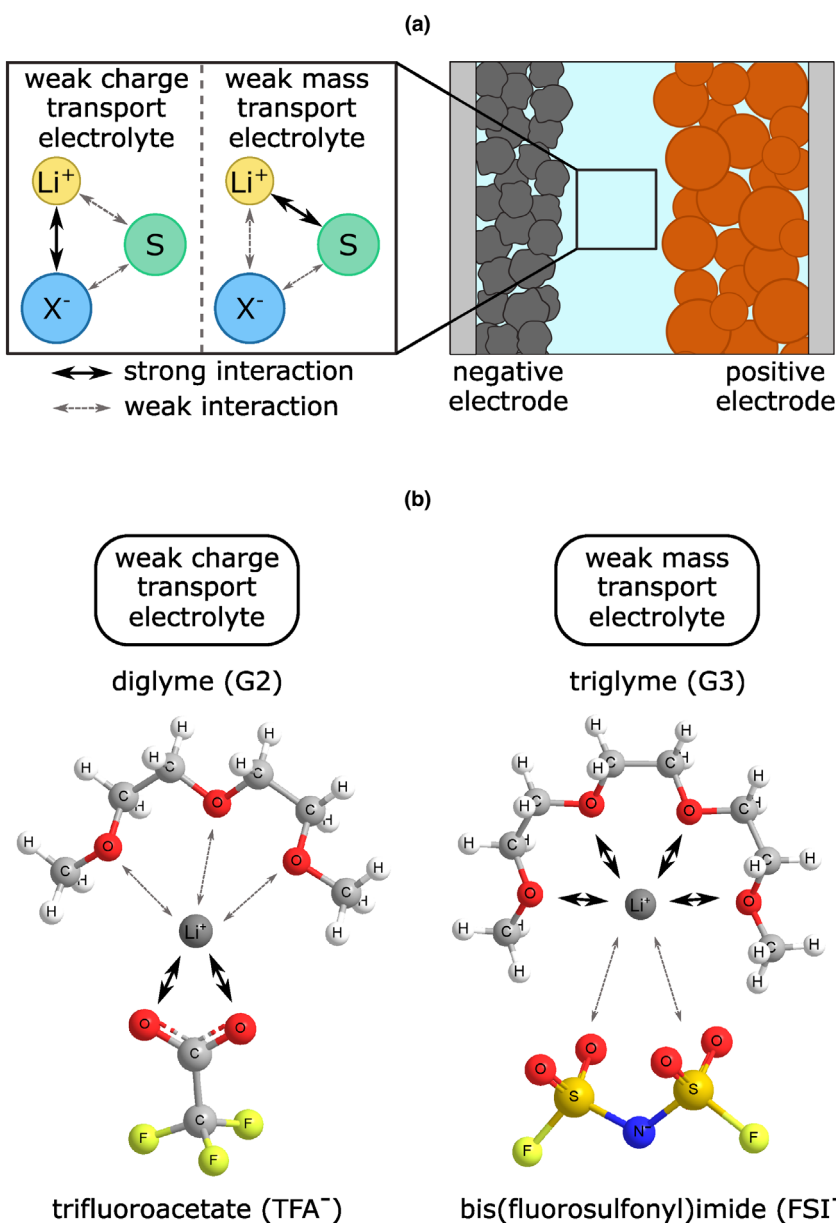


**Figure 1.** a) Schematic illustration of the interactions between  $\text{Li}^+$  ions, anions  $\text{X}^-$  and solvent molecules  $\text{S}$  in weak charge transport electrolytes as compared to weak mass transport electrolytes for lithium-ion batteries. b) Examples for weak mass transport and weak charge transport electrolytes with illustration of interactions.

weakly coordinating anions, such as bis(fluorosulfonyl)imide ( $\text{FSI}^-$ ), see Figure 1b.

In Roling et al.<sup>[33]</sup> we gave a short sketch of the theoretical background of this classification in the case of 1–1 electrolytes (univalent cation, univalent anion). In this paper, a comprehensive theoretical framework for this classification is presented, which is valid for electrolytes with a single dissolved salt with arbitrary ionic charge numbers. The Onsager transport formalism is combined with linear response theory for relating equilibrium center-of-mass fluctuations and collective translational dipole fluctuations of the ions to the transport properties in battery cells. The classification approach is substantiated by showing

that both fast charge transport and fast mass transport are indispensable for fast  $\text{Li}^+$  transport under anion-blocking conditions in lithium-ion batteries. Furthermore, we consider the influence of cross correlations between center-of-mass and collective translational dipole fluctuations on the transport properties, which were neglected in Roling et al.<sup>[33]</sup>

## 2. General Theoretical Framework Based on Onsager Formalism and Linear Response Theory

An electrolyte solution is considered containing cations with mass of  $m_+$  and charge  $q_+ = z_+ \cdot e$  as well as anions with mass of  $m_-$  and charge  $q_- = z_- \cdot e$ . Here,  $z_{\pm}$  and  $e = 1.6 \cdot 10^{-19}$  C denote the ionic charge numbers and the elementary charge, respectively. The stoichiometric factor of cations and anions,  $\nu_+$  and  $\nu_-$ , are related to the charge numbers via  $\nu_+ \cdot z_+ = |\nu_- \cdot z_-|$ . The mass ratio of the ions is defined as:  $k = m_-/m_+$ .

In thermal equilibrium, movements of an ion  $i$  within a time interval  $t$  can be described by a displacement vector

$$\Delta \vec{R}_i(t) = \begin{pmatrix} \Delta x_i(t) \\ \Delta y_i(t) \\ \Delta z_i(t) \end{pmatrix}. \quad \text{The time interval } t \text{ is chosen such that the ion dynamics is diffusive, that is, } \Delta \vec{R}_i(t) \propto t. \text{ The time-dependent displacement vector of a cation } i \text{ in } x \text{ direction is denoted by } \Delta R_i^{\rightarrow+}, \text{ while the time-dependent displacement vector of an anion } i \text{ in } x \text{ direction is denoted by } \Delta R_i^{\rightarrow-}.$$

$t$  is chosen such that the ion dynamics is diffusive, that is,  $\Delta \vec{R}_i(t) \propto t$ . The time-dependent displacement vector of a cation  $i$  in  $x$  direction is denoted by  $\Delta R_i^{\rightarrow+}$ , while the time-dependent displacement vector of an anion  $i$  in  $x$  direction is denoted by  $\Delta R_i^{\rightarrow-}$ .

### 2.1. Definition of Center-of-Mass Fluctuations and Collective Translational Dipole Fluctuations in Equilibrium

The ionic displacements lead to center-of-mass fluctuations  $\Delta \vec{R}_{\text{CM}}(t)$  and collective translational dipole fluctuations  $e \cdot \Delta \vec{R}_{\text{DP}}(t)$  of the ions, which are given by:

$$\Delta \vec{R}_{\text{CM}}(t) = \frac{1}{1+k} \cdot \sum_i \Delta \vec{R}_i^{\rightarrow+}(t) + \frac{k}{1+k} \cdot \sum_i \Delta \vec{R}_i^{\rightarrow-}(t) \quad (1)$$

$$e \cdot \Delta \vec{R}_{\text{DP}}(t) = z_+ e \cdot \sum_i \Delta \vec{R}_i^{\rightarrow+}(t) + z_- e \cdot \sum_i \Delta \vec{R}_i^{\rightarrow-}(t) \quad (2)$$

We note that the center-of-mass  $\Delta \vec{R}_{\text{CM}}(t)$  refers to the system of all individual ions in the sample.

Solving Equations (3) and (4) for  $\sum_i \Delta \vec{R}_i^+(t)$  and  $\sum_i \Delta \vec{R}_i^-(t)$  results in:

$$\sum_i \Delta \vec{R}_i^+(t) = \frac{k}{k \cdot z_+ - z_-} \cdot \Delta \vec{R}_{DP}(t) - \frac{z_-(1+k)}{k \cdot z_+ - z_-} \cdot \Delta \vec{R}_{CM}(t) \quad (3)$$

$$\sum_i \Delta \vec{R}_i^-(t) = -\frac{1}{k \cdot z_+ - z_-} \cdot \Delta \vec{R}_{DP}(t) + \frac{z_+(1+k)}{k \cdot z_+ - z_-} \cdot \Delta \vec{R}_{CM}(t) \quad (4)$$

### 2.2. Transport Coefficients and Mobility-Based Cation Transference Number Derived from Linear Response Theory

Now we use Equations (3) and (4) to calculate the Onsager coefficients  $\sigma_{++}$ ,  $\sigma_{--}$ , and  $\sigma_{+-}$  in the framework of linear response theory:<sup>[34]</sup>

$$\begin{aligned} \sigma_{++} &= \lim_{t \rightarrow \infty} \frac{e^2}{6V \cdot k_B T \cdot t} \cdot \left\langle \left( \sum_i z_+ \cdot \Delta \vec{R}_i^+(t) \right)^2 \right\rangle \\ &= \lim_{t \rightarrow \infty} \frac{z_+^2 \cdot e^2}{6V \cdot k_B T \cdot t} \cdot \left[ \left( \frac{k}{k \cdot z_+ - z_-} \right)^2 \cdot \left\langle \Delta \vec{R}_{DP}(t)^2 \right\rangle - 2 \cdot \frac{k \cdot z_-(1+k)}{(k \cdot z_+ - z_-)^2} \right. \\ &\quad \left. \cdot \left\langle \Delta \vec{R}_{DP}(t) \cdot \Delta \vec{R}_{CM}(t) \right\rangle + \left( \frac{z_-(1+k)}{k \cdot z_+ - z_-} \right)^2 \cdot \left\langle \Delta \vec{R}_{CM}(t)^2 \right\rangle \right] \end{aligned} \quad (5)$$

$$\begin{aligned} \sigma_{--} &= \lim_{t \rightarrow \infty} \frac{e^2}{6V \cdot k_B T \cdot t} \cdot \left\langle \left( \sum_i z_- \cdot \Delta \vec{R}_i^-(t) \right)^2 \right\rangle \\ &= \lim_{t \rightarrow \infty} \frac{z_-^2 \cdot e^2}{6V \cdot k_B T \cdot t} \cdot \left[ \left( \frac{1}{k \cdot z_+ - z_-} \right)^2 \cdot \left\langle \Delta \vec{R}_{DP}(t)^2 \right\rangle - 2 \right. \\ &\quad \left. \cdot \frac{z_+(1+k)}{(k \cdot z_+ - z_-)^2} \cdot \left\langle \Delta \vec{R}_{DP}(t) \cdot \Delta \vec{R}_{CM}(t) \right\rangle + \left( \frac{z_+(1+k)}{k \cdot z_+ - z_-} \right)^2 \cdot \left\langle \Delta \vec{R}_{CM}(t)^2 \right\rangle \right] \end{aligned} \quad (6)$$

$$\begin{aligned} \sigma_{+-} &= -\lim_{t \rightarrow \infty} \frac{e^2}{6V \cdot k_B T \cdot t} \cdot \left\langle \sum_i z_+ \cdot \Delta \vec{R}_i^+(t) \cdot \sum_i z_- \cdot \Delta \vec{R}_i^-(t) \right\rangle \\ &= -\lim_{t \rightarrow \infty} \frac{z_+ \cdot z_- \cdot e^2}{6V \cdot k_B T \cdot t} \cdot \left[ -\frac{k}{(k \cdot z_+ - z_-)^2} \cdot \left\langle \Delta \vec{R}_{DP}(t)^2 \right\rangle \right. \\ &\quad \left. + \frac{(z_- + z_+ \cdot k)(1+k)}{(k \cdot z_+ - z_-)^2} \cdot \left\langle \Delta \vec{R}_{DP}(t) \cdot \Delta \vec{R}_{CM}(t) \right\rangle - \frac{z_+ \cdot z_- \cdot (1+k)^2}{(k \cdot z_+ - z_-)^2} \cdot \left\langle \Delta \vec{R}_{CM}(t)^2 \right\rangle \right] \end{aligned} \quad (7)$$

In Equations (5)–(7),  $\langle \rangle$  denotes the ensemble average. The ionic conductivity  $\sigma_{ion}$  is then given by:

$$\sigma_{ion} = \sigma_{++} + \sigma_{--} - 2 \cdot \sigma_{+-} = \lim_{t \rightarrow \infty} \frac{e^2}{6V \cdot k_B T \cdot t} \cdot \left\langle \Delta \vec{R}_{DP}(t)^2 \right\rangle \quad (8)$$

As well-known,<sup>[35,36]</sup> the ionic conductivity is exclusively determined by collective translational dipole fluctuation of the ions in equilibrium.

Considering Equations (5)–(8) we define two additional transport coefficients:

$$\sigma_{mass} \equiv \lim_{t \rightarrow \infty} \frac{e^2}{6V \cdot k_B T \cdot t} \cdot \left\langle \Delta \vec{R}_{CM}(t)^2 \right\rangle \quad (9)$$

$$\sigma_{corr} \equiv \lim_{t \rightarrow \infty} \frac{e^2}{6V \cdot k_B T \cdot t} \cdot \left\langle \Delta \vec{R}_{DP}(t) \cdot \Delta \vec{R}_{CM}(t) \right\rangle \quad (10)$$

As will be shown below,  $\sigma_{mass}$  describes mass transport in the electrolyte, that is, the transport of neutral salt in the presence a chemical potential gradient of the salt. Consequently,  $\sigma_{mass}$  is clearly distinct from the so-called Nernst-Einstein conductivity calculated from the self-diffusion coefficients of the ions.<sup>[37]</sup> The quantity  $\sigma_{corr}$  describes the influence of cross correlations between collective translational dipole fluctuations and center-of-mass fluctuations on transport. This influence will be analyzed in Section 4.

Using Equations (8)–(10), the Onsager coefficients can be rewritten as:

$$\begin{aligned} \sigma_{++} &= \left( \frac{z_+ \cdot k}{k \cdot z_+ - z_-} \right)^2 \cdot \sigma_{ion} - 2 \cdot \frac{z_+^2 \cdot z_- \cdot k \cdot (1+k)}{(k \cdot z_+ - z_-)^2} \cdot \sigma_{corr} \\ &\quad + \left( \frac{z_+ \cdot z_- \cdot (1+k)}{k \cdot z_+ - z_-} \right)^2 \cdot \sigma_{mass} \end{aligned} \quad (11)$$

$$\begin{aligned} \sigma_{--} &= \left( \frac{z_-}{k \cdot z_+ - z_-} \right)^2 \cdot \sigma_{ion} - 2 \cdot \frac{z_-^2 \cdot z_+ \cdot (1+k)}{(k \cdot z_+ - z_-)^2} \cdot \sigma_{corr} \\ &\quad + \left( \frac{z_+ \cdot z_- \cdot (1+k)}{k \cdot z_+ - z_-} \right)^2 \cdot \sigma_{mass} \end{aligned} \quad (12)$$

$$\begin{aligned} \sigma_{+-} &= \frac{z_+ \cdot z_- \cdot k}{(k \cdot z_+ - z_-)^2} \cdot \sigma_{ion} - \frac{z_+ \cdot z_- \cdot (z_- + k \cdot z_+) \cdot (1+k)}{(k \cdot z_+ - z_-)^2} \cdot \sigma_{corr} \\ &\quad + \left( \frac{z_+ \cdot z_- \cdot (1+k)}{k \cdot z_+ - z_-} \right)^2 \cdot \sigma_{mass} \end{aligned} \quad (13)$$

The mobility-based cation transference number is then given by:

$$\begin{aligned} t_+^{\mu} &= \frac{\sigma_{++} - \sigma_{+-}}{\sigma_{ion}} \\ &= \frac{z_+^2 \cdot k^2 - z_+ \cdot z_- \cdot k}{(k \cdot z_+ - z_-)^2} + \frac{z_+ \cdot z_- \cdot (z_- - z_+ \cdot k)(1+k)}{(k \cdot z_+ - z_-)^2} \cdot \frac{\sigma_{corr}}{\sigma_{ion}} \end{aligned} \quad (14)$$

### 2.3. Onsager Reciprocal Relations for Cation and Anion Flux

According to the Onsager reciprocal relations, the molar fluxes of the cations,  $J_+$ , and of the anions,  $J_-$ , can be written as:

$$J_+ = -\left( \frac{\sigma_{++}}{z_+^2 \cdot F^2} \frac{d\tilde{\mu}_+}{dx} - \frac{\sigma_{+-}}{z_+ \cdot z_- \cdot F^2} \frac{d\tilde{\mu}_-}{dx} \right) \quad (15)$$

$$J_- = -\left( \frac{\sigma_{--}}{z_-^2 \cdot F^2} \frac{d\tilde{\mu}_-}{dx} - \frac{\sigma_{+-}}{z_+ \cdot z_- \cdot F^2} \frac{d\tilde{\mu}_+}{dx} \right) \quad (16)$$

The gradients of the electrochemical potential of the ions are the driving forces and are defined as:

$$\frac{d\tilde{\mu}_i}{dx} = z_i \cdot F \cdot \frac{d\varphi}{dx} + R \cdot T \cdot \frac{d\ln a_{\pm}}{dx} \quad (17)$$

Here,  $\varphi$  is the electric potential, and  $a_{\pm} = \nu_+ \nu_- \sqrt{a_+^{\nu_+} \cdot a_-^{\nu_-}}$  denotes the mean activity of the ions.  $a_+$  and  $a_-$  are the individual activities of cations and anions, respectively.

## 2.4. Cation Flux under Anion-Blocking Conditions

When an electrolyte is placed between two cation-reversible and anion-blocking electrodes with spacing  $d$ , a salt concentration gradient and an electric gradient are formed, such that anion migration and anion diffusion cancel out. This implies that  $J_- = 0$ . With Equations (16) and (17) it follows that:

$$\frac{d\varphi}{dx} = \frac{RT}{F} \cdot \frac{z_- \cdot \sigma_{+-} - \sigma_{--} \cdot z_+}{z_+ \cdot z_- \cdot (\sigma_{--} - \sigma_{+-})} \cdot \frac{d\ln a_{\pm}}{dx} \quad (18)$$

Integration of Equation (18) leads to the following expression for the electric potential drop over the bulk of the electrolyte in the case of anion-blocking conditions (index abc):

$$\Delta\varphi_{\text{bulk}}^{\text{abc}} = \frac{RT}{F} \cdot \frac{z_- \cdot \sigma_{+-} - \sigma_{--} \cdot z_+}{z_+ \cdot z_- \cdot (\sigma_{--} - \sigma_{+-})} \cdot \Delta\ln a_{\pm} \quad (19)$$

The Nernst potential drop over the interfaces between the electrolyte and the cation-reversible electrodes is given by:

$$\Delta\varphi_{\text{Nernst}} = \frac{RT}{z_+ F} \cdot \Delta\ln a_{\pm} \quad (20)$$

When we now normalize the overall potential drop between the electrodes to the electrode spacing  $d$ , we obtain:

$$\begin{aligned} \frac{\Delta\varphi^{\text{abc}}}{d} &= \frac{\Delta\varphi_{\text{bulk}}^{\text{abc}} + \Delta\varphi_{\text{Nernst}}}{d} \\ &= \frac{RT}{z_+ \cdot F} \cdot \left( \frac{z_- \cdot \sigma_{+-} - \sigma_{--} \cdot z_+}{z_- \cdot (\sigma_{--} - \sigma_{+-})} + 1 \right) \cdot \frac{\Delta\ln a_{\pm}}{d} \\ &= \frac{RT}{F} \cdot \left( \frac{(z_- - z_+) \cdot \sigma_{--}}{z_+ \cdot z_- \cdot (\sigma_{--} - \sigma_{+-})} \right) \cdot \frac{\Delta\ln a_{\pm}}{d} \\ &= \frac{RT}{F} \cdot \left( \frac{(z_- - z_+) \cdot \sigma_{--}}{z_+ \cdot z_- \cdot (\sigma_{--} - \sigma_{+-})} \right) \cdot \frac{d\ln a_{\pm}}{dx} \end{aligned} \quad (21)$$

The cation flux is obtained by combining Equations (15) and (17):

$$j^{\text{abc}} = z_+ \cdot F \cdot J_+^{\text{abc}} = -(\sigma_{++} - \sigma_{+-}) \cdot \frac{d\varphi}{dx} - \left( \frac{\sigma_{++}}{z_+} - \frac{\sigma_{+-}}{z_-} \right) \cdot \frac{RT}{F} \cdot \frac{d\ln a_{\pm}}{dx} \quad (22)$$

Taking into account Equations (18) and (21) results in:

$$\begin{aligned} j^{\text{abc}} &= \frac{(z_- - z_+) \cdot (\sigma_{++} \cdot \sigma_{--} - \sigma_{+-}^2)}{z_+ \cdot z_- \cdot (\sigma_{--} - \sigma_{+-}) \sigma_{--}} \cdot \frac{RT}{F} \cdot \frac{d\ln a_{\pm}}{dx} \\ &= \frac{\sigma_{++} \cdot \sigma_{--} - \sigma_{+-}^2}{\sigma_{--}} \cdot \frac{\Delta\varphi^{\text{abc}}}{d} \equiv \sigma^{\text{abc}} \cdot \frac{\Delta\varphi^{\text{abc}}}{d} \end{aligned} \quad (23)$$

Consequently, the cation conductivity  $\sigma^{\text{abc}}$  under anion-blocking conditions and the related cation transference number  $t_+^{\text{abc}}$  are given by:

$$\sigma^{\text{abc}} = \frac{\sigma_{++} \cdot \sigma_{--} - \sigma_{+-}^2}{\sigma_{--}} \quad (24)$$

$$t_+^{\text{abc}} = \frac{\sigma^{\text{abc}}}{\sigma_{\text{ion}}} = \frac{\sigma_{++} \cdot \sigma_{--} - \sigma_{+-}^2}{\sigma_{--} \cdot \sigma_{\text{ion}}} \quad (25)$$

## 2.5. Neutral Salt Transport

Neutral salt transport with zero electrical current flow  $j = 0$  implies that:

$$z_+ \cdot J_+ = -z_- \cdot J_- \quad (26)$$

Taking into account Equations (15)–(17) results in:

$$\frac{d\varphi}{dx} = -\frac{RT}{F} \cdot \frac{d\ln a_{\pm}}{dx} \left( \frac{z_+ \cdot \sigma_{--} + z_- \cdot \sigma_{++} - (z_+ + z_-) \cdot \sigma_{+-}}{z_+ \cdot z_- \cdot \sigma_{\text{ion}}} \right) \quad (27)$$

Inserting Equation (27) into Equation (15) combined with Equation (17) leads to the following expression for the salt flux:

$$\begin{aligned} J_{\text{salt}} &= \frac{J_+}{\nu_+} = -\frac{1}{\nu_+ \cdot z_+^2 \cdot z_- \cdot F^2} (z_- - z_+) \cdot \\ &RT \cdot \frac{d\ln a_{\pm}}{dx} \left( \frac{\sigma_{++} \cdot \sigma_{--} - \sigma_{+-}^2}{\sigma_{\text{ion}}} \right) \end{aligned} \quad (28)$$

With  $(z_- - z_+) = z_+ \cdot (\nu_+ + \nu_-) / \nu_-$  and  $d\mu_{\text{salt}} = RT \cdot d\ln a_{\text{salt}} = RT \cdot (\nu_+ + \nu_-) \cdot d\ln a_{\pm}$ , Equation (28) can be rewritten as:

$$J_{\text{salt}} = -\frac{1}{\nu_+ \cdot \nu_- \cdot z_+ \cdot z_- \cdot F^2} \cdot \left( \frac{\sigma_{++} \cdot \sigma_{--} - \sigma_{+-}^2}{\sigma_{\text{ion}}} \right) \cdot \frac{d\mu_{\text{salt}}}{dx} \quad (29)$$

With the Onsager definition

$$J_{\text{salt}} = -\frac{\sigma_{\text{salt}}}{z_+ \cdot z_- \cdot F^2} \cdot \frac{d\mu_{\text{salt}}}{dx} \quad (30)$$

the following expression for the salt transport coefficient  $\sigma_{\text{salt}}$  is obtained:

$$\sigma_{\text{salt}} = \frac{1}{\nu_+ \cdot \nu_-} \cdot \left( \frac{\sigma_{++} \cdot \sigma_{--} - \sigma_{+-}^2}{\sigma_{\text{ion}}} \right) \quad (31)$$

## 3. General Relations for 1-1-Electrolytes

For a 1-1-electrolyte containing univalent cations and univalent anions, we have  $\nu_+ = 1$ ,  $\nu_- = 1$ ,  $z_+ = 1$ , and  $z_- = -1$ . In this case, Equations (11)–(14) for the Onsager coefficients and for the mobility-based cation transference number simplify to:

$$\sigma_{++} = \left( \frac{k}{1+k} \right)^2 \cdot \sigma_{\text{ion}} + \frac{2k}{1+k} \cdot \sigma_{\text{corr}} + \sigma_{\text{mass}} \quad (32)$$

$$\sigma_{--} = \left( \frac{1}{1+k} \right)^2 \cdot \sigma_{\text{ion}} - \frac{2}{1+k} \cdot \sigma_{\text{corr}} + \sigma_{\text{mass}} \quad (33)$$

$$\sigma_{+-} = -\frac{k}{(1+k)^2} \cdot \sigma_{\text{ion}} + \frac{k-1}{1+k} \cdot \sigma_{\text{corr}} + \sigma_{\text{mass}} \quad (34)$$

$$t_{+}^{\mu} = \frac{\sigma_{++} - \sigma_{+-}}{\sigma_{\text{ion}}} = \frac{k}{1+k} + \frac{\sigma_{\text{corr}}}{\sigma_{\text{ion}}} \quad (35)$$

Equation (31) for the salt transport coefficient  $\sigma_{\text{salt}}$  simplifies to:

$$\sigma_{\text{salt}} = \frac{\sigma_{++} \cdot \sigma_{--} - \sigma_{+-}^2}{\sigma_{\text{ion}}} \quad (36)$$

Inserting Equations (32)–(34) into (36) yields:

$$\sigma_{\text{salt}} = \sigma_{\text{mass}} - \frac{(\sigma_{\text{corr}})^2}{\sigma_{\text{ion}}} \quad (37)$$

Equations (24) and (25) for the effective cation conductivity  $\sigma^{\text{abc}}$  and for the cation transference number  $t_{+}^{\text{abc}}$  under anion-blocking conditions are also valid for 1–1 electrolytes.

Inserting Equations (33) and (37) into (24) yields:

$$\begin{aligned} \sigma^{\text{abc}} &= \frac{\sigma_{++} \cdot \sigma_{--} - \sigma_{+-}^2}{\sigma_{--}} = \frac{\sigma_{\text{mass}} \cdot \sigma_{\text{ion}} - \sigma_{\text{corr}}^2}{\left(\frac{1}{1+k}\right)^2 \cdot \sigma_{\text{ion}} - \frac{2}{1+k} \cdot \sigma_{\text{corr}} + \sigma_{\text{mass}}} \\ &= \frac{(1+k)^2 \cdot \sigma_{\text{mass}} \cdot \sigma_{\text{ion}} - (1+k)^2 \cdot \sigma_{\text{corr}}^2}{\sigma_{\text{ion}} - 2(1+k) \cdot \sigma_{\text{corr}} + (1+k)^2 \cdot \sigma_{\text{mass}}} \end{aligned} \quad (38)$$

#### 4. Influence of Transport Coefficient $\sigma_{\text{corr}}$ on Mass Transport in Weak Charge Transport Electrolytes and in Weak Mass Transport Electrolytes

When considering Equations (35) and (37), the question arises whether the mass transport coefficient  $\sigma_{\text{mass}}$  and the mass ratio  $k$  can be determined for an electrolyte with unknown value for  $\sigma_{\text{corr}}$ . Therefore, we analyze in the following the influence of  $\sigma_{\text{corr}}$  on the mass transport properties of weak charge transport electrolytes and of weak mass transport electrolytes.

##### 4.1. Weak Charge Transport Electrolytes

We consider an electrolyte with weak ion dissociation. When the degree of dissociation of the salt  $AX_{(\text{solv})}$  into free ions  $A_{(\text{solv})}^{+}$  and  $X_{(\text{solv})}^{-}$  is given by  $\alpha \ll 1$ , the transport coefficients of free ions and ion pairs can be written as:<sup>[34]</sup>

$$\sigma_{A^{+}} = \frac{\alpha \cdot c_{\text{salt}} \cdot F^2}{RT} \cdot D_{A^{+}}^{*} \quad (39)$$

$$\sigma_{X^{-}} = \frac{\alpha \cdot c_{\text{salt}} \cdot F^2}{RT} \cdot D_{X^{-}}^{*} \quad (40)$$

$$s = \frac{(1-\alpha) \cdot c_{\text{salt}} \cdot F^2}{RT} \cdot D_{AX}^{*} \quad (41)$$

with  $D_{A^{+}}^{*}$ ,  $D_{X^{-}}^{*}$ , and  $D_{AX}^{*}$  denoting the self-diffusion coefficients of free cations, free anions, and ion pairs, respectively.  $\alpha \ll 1$  implies that  $\sigma_{A^{+}} \ll s$  and  $\sigma_{X^{-}} \ll s$ .

In classical weak electrolyte theory, an ion pair exists, if the distance between cation and anion is smaller than the Bjerrum length.<sup>[38]</sup> From a dynamic point of view, the transport of ion pairs is relevant, if the average distance over which a cation–anion pair is transported is significantly larger than the diameters of the solvated ions.

The Onsager coefficients and the ionic conductivity for such an electrolyte are given by:<sup>[34]</sup>

$$\sigma_{++} = \sigma_{A^{+}} + s \quad (42)$$

$$\sigma_{--} = \sigma_{X^{-}} + s \quad (43)$$

$$\sigma_{+-} = s \quad (44)$$

$$\sigma_{\text{ion}} = \sigma_{A^{+}} + \sigma_{X^{-}} \quad (45)$$

Now we calculate the salt transport coefficient  $\sigma_{\text{salt}}$ :

$$\begin{aligned} \sigma_{\text{salt}} &= \frac{\sigma_{++} \cdot \sigma_{--} - \sigma_{+-}^2}{\sigma_{\text{ion}}} \\ &= \frac{(\sigma_{A^{+}} + s) \cdot (\sigma_{X^{-}} + s) - s^2}{\sigma_{A^{+}} + \sigma_{X^{-}}} \\ &= \frac{(\sigma_{A^{+}} + \sigma_{X^{-}}) \cdot s + \sigma_{A^{+}} \cdot \sigma_{X^{-}}}{\sigma_{A^{+}} + \sigma_{X^{-}}} \approx s \end{aligned} \quad (46)$$

From Equations (32)–(34), it follows for the mass transport coefficient  $\sigma_{\text{mass}}$ :

$$\begin{aligned} \sigma_{\text{mass}} &= \left(\frac{1}{1+k}\right)^2 \cdot \sigma_{++} + \left(\frac{k}{1+k}\right)^2 \cdot \sigma_{--} + \frac{2k}{(1+k)^2} \cdot \sigma_{+-} \\ &= \left(\frac{1}{1+k}\right)^2 \cdot (\sigma_{A^{+}} + s) + \left(\frac{k}{1+k}\right)^2 \cdot (\sigma_{X^{-}} + s) + \frac{2k}{(1+k)^2} \cdot s \\ &= \left(\frac{1}{1+k}\right)^2 \cdot \sigma_{A^{+}} + \left(\frac{k}{1+k}\right)^2 \cdot \sigma_{X^{-}} + s \approx s \end{aligned} \quad (47)$$

Since  $\sigma_{\text{salt}}$  and  $\sigma_{\text{mass}}$  are virtually identical, the term  $(\sigma_{\text{corr}})^2/\sigma_{\text{ion}}$  must be negligible. This can also be seen when calculating  $\sigma_{\text{corr}}$  from Equations (32)–(34):

$$\begin{aligned} \sigma_{\text{corr}} &= \frac{1}{1+k} \cdot \sigma_{++} - \frac{k}{1+k} \cdot \sigma_{--} + \frac{k-1}{1+k} \cdot \sigma_{+-} \\ &= \frac{1}{1+k} \cdot \sigma_{A^{+}} - \frac{k}{1+k} \cdot \sigma_{X^{-}} \ll \sigma_{\text{salt}} \approx s \end{aligned} \quad (48)$$

From this we conclude that for weak charge transport electrolytes, the mass transport coefficient  $\sigma_{\text{mass}}$  can be safely identified with the salt transport coefficient  $\sigma_{\text{salt}}$ . However, the transport data yield no information about the mass ratio  $k$ .

##### 4.2. Weak Mass Transport Electrolytes

Weak mass transport electrolytes are characterized by  $\sigma_{\text{mass}} \ll \sigma_{\text{ion}}$ . In order to derive information about  $\sigma_{\text{corr}}$ , two weak mass transport electrolytes are considered with inverse mass ratio  $k_1$  and  $k_2 = 1/k_1$  and otherwise identical properties. For symmetry reasons, these electrolytes exhibit the same values for  $\sigma_{\text{ion}}$ ,  $\sigma_{\text{mass}}$  and  $\sigma_{+-}$ . With Equation (34) this implies that:

$$\begin{aligned}\sigma_{+-} &= -\frac{k_1}{(1+k_1)^2} \cdot \sigma_{\text{ion}} + \frac{k_1-1}{1+k_1} \cdot \sigma_{\text{corr}}(k_1) + \sigma_{\text{mass}} \\ &= -\frac{1/k_1}{(1+1/k_1)^2} \cdot \sigma_{\text{ion}} + \frac{1/k_1-1}{1+1/k_1} \cdot \sigma_{\text{corr}}(1/k_1) + \sigma_{\text{mass}}\end{aligned}\quad (49)$$

From Equation (49) it follows that:

$$\begin{aligned}\frac{k_1-1}{1+k_1} \cdot \sigma_{\text{corr}}(k_1) &= \frac{1-k_1}{1+k_1} \cdot \sigma_{\text{corr}}(1/k_1) \\ \rightarrow \sigma_{\text{corr}}(k_1) &= -\sigma_{\text{corr}}(1/k_1)\end{aligned}\quad (50)$$

Equation (50) implies that for identical ion masses, that is, for  $k = 1$ , correlations between dipole and center-of-mass fluctuation are absent, that is,  $\sigma_{\text{corr}} = 0$ .

Next, the limits  $k \rightarrow \infty$  and  $k \rightarrow 0$  are considered. In these limits, one type of ion moves much faster than the other type, so that cation–anion correlations become negligible, that is,  $\sigma_{+-} \rightarrow 0$ . Taking into account Equation (34),  $k \rightarrow \infty$  leads to  $\sigma_{\text{corr}} = -\sigma_{\text{mass}}$  and  $k \rightarrow 0$  leads to  $\sigma_{\text{corr}} = \sigma_{\text{mass}}$ . Consequently, the following relation

$$|\sigma_{\text{corr}}| \leq \sigma_{\text{mass}}\quad (51)$$

is generally valid. Together with  $\sigma_{\text{mass}} \ll \sigma_{\text{ion}}$ , this implies that the  $\sigma_{\text{corr}}$ -containing terms in Equations (35) and (37) can be safely neglected for weak mass transport electrolytes.

## 5. Electrolyte Classification and Assessment of Transport Properties in Batteries

In Roling et al.,<sup>[33]</sup> a general electrolyte classification based on comparing charge and mass transport was suggested. The molar mass transport coefficient  $\Lambda_{\text{mass}} = \sigma_{\text{salt}}/c_{\text{salt}}$  was plotted versus the molar ionic conductivity  $\Lambda_{\text{charge}} = \sigma_{\text{ion}}/c_{\text{salt}}$ , and it was shown that the transport data of an ideal strong electrolyte with negligible ion-ion interactions are characterized by  $\Lambda_{\text{mass}} = \frac{k^2}{(1+k)^2} \cdot \Lambda_{\text{charge}}$ . For  $k$  values close to unity, this can be approximated by  $\Lambda_{\text{mass}} \approx \frac{1}{4} \cdot \Lambda_{\text{charge}}$ . Electrolytes with strong charge transport limitations, that is,  $\frac{1}{4} \cdot \Lambda_{\text{charge}} \ll \Lambda_{\text{mass}}$ , were termed as “weak charge transport electrolytes,” whereas electrolytes with strong mass transport limitations, that is,  $\Lambda_{\text{mass}} \ll \frac{1}{4} \cdot \Lambda_{\text{charge}}$ , were termed as “weak mass transport electrolytes.”

In the following, we relate this classification to the transport properties of a  $\text{Li}^+$  electrolyte in a lithium-ion battery. During the cycling of such a battery, the  $\text{Li}^+$  ions are transported under anion-blocking conditions described by the transport coefficient  $\sigma^{\text{abc}} = t_{+}^{\text{abc}} \cdot \sigma_{\text{ion}} = \frac{\sigma_{++} \cdot \sigma_{--} - \sigma_{+-}^2}{\sigma_{--}} = \frac{\sigma_{\text{salt}}}{\sigma_{--}}$ , see Equations (36) and (38). In this expression, specific transport coefficients  $\sigma_{\text{ion}}$  and  $\sigma_{\text{salt}}$  appear and not their molar counterparts. Consequently, in **Figure 2**, we plot  $\sigma_{\text{salt}}$  versus  $\sigma_{\text{ion}}$  for different electrolyte solutions, and we add iso- $\sigma^{\text{abc}}$  lines to this plot with two specific  $\sigma^{\text{abc}}$  values. The first value  $\sigma_{\text{standard}}^{\text{abc}} = 3.5 \text{ mS cm}^{-1}$  is an estimate for standard carbonate-based battery electrolytes with ionic conductivities in the range of  $\sigma_{\text{ion}} = 10 \text{ mS cm}^{-1}$  and with  $\text{Li}^+$  transference numbers in the range of 0.35.<sup>[39]</sup> These electrolytes enable fast  $\text{Li}^+$  ion transport in the battery. The second value is based on the assumption that  $\sigma^{\text{abc}}$  should not fall below a value of  $\sigma_{\text{min}}^{\text{abc}} = 1 \text{ mS cm}^{-1}$  in order to ensure sufficiently fast  $\text{Li}^+$  ion transport. Of course, this value can be adjusted to the specific requirements of a battery under consideration. In **Figure 2**,

we use a background color code with green in case of  $\sigma^{\text{abc}} \geq \sigma_{\text{standard}}^{\text{abc}}$ , yellow in case of  $\sigma_{\text{standard}}^{\text{abc}} > \sigma^{\text{abc}} \geq \sigma_{\text{min}}^{\text{abc}}$  and red in case of  $\sigma^{\text{abc}} < \sigma_{\text{min}}^{\text{abc}}$ . The plot contains also an ideal strong electrolyte line with  $\sigma_{\text{salt}} = \frac{1}{4} \cdot \sigma_{\text{ion}}$ .

The color code reveals that for achieving sufficiently high value of  $\sigma^{\text{abc}}$ , both the ionic conductivity  $\sigma_{\text{ion}}$  and the salt transport coefficient  $\sigma_{\text{salt}}$  must be sufficiently high. This can also be seen from Equation (38), which in case of  $k \approx 1$  and  $\sigma_{\text{corr}} < \sigma_{\text{mass}}$  can be approximated by:

$$\sigma^{\text{abc}} = \frac{\sigma_{++} \cdot \sigma_{--} - \sigma_{+-}^2}{\sigma_{--}} \approx \frac{\sigma_{\text{salt}} \cdot \sigma_{\text{ion}}}{\frac{1}{4} \sigma_{\text{ion}} + \sigma_{\text{salt}}}\quad (52)$$

In **Figure 2** we show  $\sigma_{\text{salt}}$  versus  $\sigma_{\text{ion}}$  data points for a number of  $\text{Li}^+$  electrolytes, for which reliable Onsager coefficients either from experiment or from MD simulations are available in the literature. As seen from the figure, only a fraction of the data points is located in the green or in the yellow regime. The data point for a 0.95 M solution of  $\text{LiPF}_6$  in a carbonate-based electrolyte (EC:EMC with molar ratio of 27:73) is clearly in the green regime. However, it is important to note that this data point is based on a MD simulation at 333 K.<sup>[40]</sup> At room temperature, the ion dynamics is slower and the data point is expected to be located close to the boundary between the green and the yellow regime. For the water-in-salt electrolytes  $\text{LiTFSI}/\text{H}_2\text{O}$ , the ionic conductivity  $\sigma_{\text{ion}}$  as well as the salt transport coefficient  $\sigma_{\text{salt}}$  are maximal at a molar salt concentration of  $2.3 \text{ mol L}^{-1}$ .<sup>[41]</sup> With increasing salt concentration, the ionic conductivity  $\sigma_{\text{ion}}$  drops, but the salt transport coefficient  $\sigma_{\text{salt}}$  drops even more strongly, so that the data points for high concentrations fall into the “weak mass transport electrolyte” regime. This implies that despite the fast ion dynamics in these water-in-salt electrolytes, mass transport limitations at very high salt concentration hinder fast  $\text{Li}^+$  transport under anion-blocking conditions in a lithium-ion battery. The data points for the electrolytes  $\text{LiTFSI}/\text{G4}$  are close to those of the  $\text{LiTFSI}/\text{H}_2\text{O}$  electrolytes and show a qualitatively similar concentration dependence. However, it is important to note that these data points were obtained from molecular dynamics simulations at 373 K.<sup>[42]</sup> At room temperature, the ion dynamics and transport in these electrolytes is much slower, as also seen from the experimental data points of  $\text{LiFSI}/\text{G4}$ .<sup>[43]</sup> These data points for salt concentrations between  $1.72$  and  $3.23 \text{ mol L}^{-1}$  are in the red regime and are located considerably below the ideal strong electrolyte line. This implies that  $\text{Li}^+$  transport in a battery is strongly hindered by slow mass transport. In contrast, the data points for  $\text{LiTFSI}/\text{sulfolane}$  electrolyte solutions are close to the ideal strong electrolyte lines.<sup>[44]</sup> However, the overall ion dynamics in these electrolytes is relatively slow, leading to relatively low values of both  $\sigma_{\text{ion}}$  and  $\sigma_{\text{salt}}$  (red regime). The data points for the two electrolytes  $\text{LiBF}_4/\text{G4}$  and  $\text{LiOTf}/\text{G3}$  are located above the ideal strong electrolyte line despite the high salt concentration of almost  $4 \text{ mol L}^{-1}$  and the molar ratio of salt to solvent of 1:1.<sup>[45]</sup> This gives indication that the interactions between  $\text{Li}^+$  ions and the anions ( $\text{BF}_4^-$  or  $\text{OTf}^-$ ) are stronger than the interactions between  $\text{Li}^+$  ions and glyme molecules (G3 or G4), resulting in charge transport limitations, which are slightly stronger than the mass transport limitations. Overall, charge transport and mass transport are rather slow, so that the data points of two electrolytes are located in the red regime.

Overall, our analysis reveals the following prerequisites for fast  $\text{Li}^+$  ion transport in a concentrated electrolyte solution under anion-

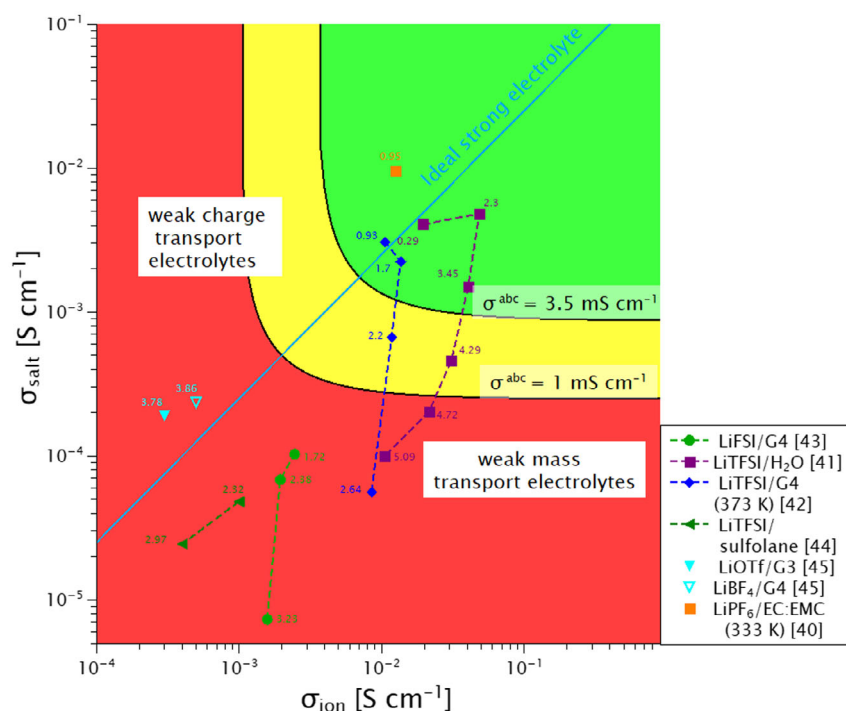


**Figure 2.** Plot of the salt transport coefficient  $\sigma_{\text{salt}}$  versus the ionic conductivity  $\sigma_{\text{ion}}$  for different  $\text{Li}^+$  electrolyte solutions. The salt concentration of the respective solution in  $\text{mol L}^{-1}$  is given as a number at the data point. If not specified otherwise, the data points originate from experiments or simulations at room temperature. The blue line refers to the transport properties of an ideal strong electrolyte with negligible ion-ion interactions. Two iso- $\sigma^{\text{abc}}$  lines (black lines) with  $\sigma^{\text{abc}}$  values of 3.5 and 1  $\text{mS cm}^{-1}$ , respectively, are sketched for assessing the  $\text{Li}^+$  transport in the electrolyte under anion-blocking conditions in a lithium-ion battery.

blocking conditions: i) The interactions between  $\text{Li}^+$  ions and anions should be balanced with the interactions between  $\text{Li}^+$  ions and solvent molecules, such that the data point in a  $\sigma_{\text{salt}}$  versus  $\sigma_{\text{ion}}$  plots is close to the ideal strong electrolyte line. ii) Both interactions should be sufficiently weak for enabling fast ion dynamics.

Regarding the characterization of transport by experiments and simulations, it is important to realize that charge transport and mass transport properties are of equal importance.

## 6. Conclusions

We have presented a comprehensive theoretical framework for relating the equilibrium ion dynamics in an electrolyte solution to the transport properties of the electrolyte solution in a lithium-ion battery cell. By combining the Onsager transport formalism with linear response theory, we have shown that center-of-mass fluctuation of the ions govern the mass transport properties, while it is well known that collective translational dipole fluctuations of the ions govern the charge transport properties.

Based on this theoretical framework, we have suggested a general classification of electrolyte solutions by comparing the ionic conductivity  $\sigma_{\text{ion}}$  with the salt transport coefficient  $\sigma_{\text{salt}}$ . Ideal strong electrolytes with negligible ion-ion interactions are characterized by  $\sigma_{\text{salt}} = \frac{k^+}{(1+k)^2} \cdot \sigma_{\text{ion}}$ , which can be approximated by  $\sigma_{\text{salt}} \approx \frac{1}{4} \cdot \sigma_{\text{ion}}$  for ion mass ratios  $k$  close to unity. Electrolyte solutions with

$\frac{1}{4} \cdot \sigma_{\text{ion}} \ll \sigma_{\text{salt}}$  are termed as “weak charge transport electrolytes,” while electrolyte solution with  $\sigma_{\text{salt}} \ll \frac{1}{4} \cdot \sigma_{\text{ion}}$  are termed as “weak mass transport electrolytes.”

Our data analysis revealed that many highly concentrated electrolyte solutions for lithium-ion batteries are “weak mass transport electrolytes.” This is the case, when the interactions of the  $\text{Li}^+$  ions with the solvent molecules are stronger than the  $\text{Li}^+$ /anion interactions. Due to the strong  $\text{Li}^+$ /solvent interactions, the fraction of “free” solvent molecules, which are not bound to  $\text{Li}^+$  ions, is small. This hinders momentum exchange between the ions and the solvent molecules, and thus the equilibrium center-of-mass fluctuations of the ions are small.

The most relevant electrolyte transport coefficient in a lithium-ion battery is the  $\text{Li}^+$  conductivity under anion-blocking conditions,  $\sigma^{\text{abc}}$ . We have shown that high values of  $\sigma^{\text{abc}}$  can only be achieved, if both charge and mass transport are sufficiently fast. To this end, the  $\text{Li}^+$ /solvent interactions should be balanced with the  $\text{Li}^+$ /anion interactions, and both types of interactions should be sufficiently weak for allowing for fast ion dynamics. In experiments and simulations, the characterization of charge transport and mass transport is of equal importance.

## Acknowledgements

We are grateful to Prof. Andreas Heuer and Prof. Monika Schönhoff for valuable discussions. Furthermore, we thank Prof. Andreas Heuer for providing MD simulation data of 0.95 M  $\text{LiPF}_6$  in EC:DMC prior to publication. Open Access funding enabled and organized by Projekt DEAL. WOA Institution: PHILIPPS-UNIVERSITÄT MARBURG Consortia Name : Projekt DEAL

## Conflict of interest

The authors declare no conflict of interest.

## Keywords

batteries, concentrated electrolytes, linear response theory, Onsager formalism, transport

Received: August 8, 2022  
Revised: September 20, 2022  
Published online: September 22, 2022

- [1] Z. Cao, M. Hashinokuchi, T. Doi, M. Inaba, *J. Electrochem. Soc.* **2019**, 166, A82.
- [2] Y. Jie, X. Ren, R. Cao, W. Cai, S. Jiao, *Adv. Funct. Mater.* **2020**, 30, 1910777.
- [3] S. Ko, Y. Yamada, A. Yamada, *Batteries Supercaps* **2020**, 3, 910–6.
- [4] S. Perez Beltran, X. Cao, J.-G. Zhang, P. B. Balbuena, *Chem. Mater.* **2020**, 32, 5973.

- [5] G. Jiang, F. Li, H. Wang, M. Wu, S. Qi, X. Liu, S. Yang, J. Ma, *Small Struct.* **2021**, 2, 2000122.
- [6] X. Cao, H. Jia, W. Xu, J.-G. Zhang, *J. Electrochem. Soc.* **2021**, 168, 10522.
- [7] X. Ou, D. Gong, C. Han, Z. Liu, Y. Tang, *Adv. Energy Mater.* **2021**, 11, 2102498.
- [8] K. Dokko, D. Watanabe, Y. Ugata, M. L. Thomas, S. Tsuzuki, W. Shinoda, K. Hashimoto, K. Ueno, Y. Umebayashi, M. Watanabe, *J. Phys. Chem. B* **2018**, 122, 10736.
- [9] A. Nakanishi, K. Ueno, D. Watanabe, Y. Ugata, Y. Matsumae, J. Liu, M. L. Thomas, K. Dokko, M. Watanabe, *J. Phys. Chem. C* **2019**, 123, 14229.
- [10] Y. Ugata, S. Sasagawa, R. Tatara, K. Ueno, M. Watanabe, K. Dokko, *J. Phys. Chem. B* **2021**, 125, 6600.
- [11] Y. Ugata, K. Shigenobu, R. Tatara, K. Ueno, M. Watanabe, K. Dokko, *Phys. Chem. Chem. Phys.* **2021**, 23, 21419.
- [12] M. Watanabe, K. Dokko, K. Ueno, M. L. Thomas, *Bull. Chem. Soc. Jpn.* **2018**, 91, 1660.
- [13] T. Mandai, K. Yoshida, K. Ueno, K. Dokko, M. Watanabe, *Phys. Chem. Chem. Phys.* **2014**, 16, 8761.
- [14] L. Suo, O. Borodin, T. Gao, M. Olguin, J. Ho, X. Fan, C. Luo, C. Wang, K. Xu, *Science (New York, N.Y.)* **2015**, 350, 938.
- [15] V. A. Azov, K. S. Egorova, M. M. Seitkalieva, A. S. Kashin, V. P. Ananikov, *Chem. Soc. Rev.* **2018**, 47, 1250.
- [16] L. Chen, J. Zhang, Q. Li, J. Vatamanu, X. Ji, T. P. Pollard, C. Cui, S. Hou, J. Chen, C. Yang, L. Ma, M. S. Ding, M. Garaga, S. Greenbaum, H.-S. Lee, O. Borodin, K. Xu, C. Wang, *ACS Energy Lett.* **2020**, 5, 968.
- [17] J. Zheng, S. Chen, W. Zhao, J. Song, M. H. Engelhard, J.-G. Zhang, *ACS Energy Lett.* **2018**, 3, 315.
- [18] Y. Yamada, J. Wang, S. Ko, E. Watanabe, A. Yamada, *Nat. Energy* **2019**, 4, 269.
- [19] S. Lin, H. Hua, Z. Li, J. Zhao, *ACS Appl. Mater. Interfaces* **2020**, 12, 33710.
- [20] T. Li, X.-Q. Zhang, N. Yao, Y.-X. Yao, L.-P. Hou, X. Chen, M.-Y. Zhou, J.-Q. Huang, Q. Zhang, *Angew. Chem. Int. Ed. Engl.* **2021**, 133, 22865.
- [21] T. T. Hagos, B. Thirumalraj, C.-J. Huang, L. H. Abrha, T. M. Hagos, G. B. Berhe, H. K. Bezabh, J. Cherng, S.-F. Chiu, W.-N. Su, B.-J. Hwang, *ACS Appl. Mater. Interfaces* **2019**, 11, 9955.
- [22] H. J. Schoenert, *J. Phys. Chem.* **1984**, 88, 3359.
- [23] D. G. Miller, *J. Phys. Chem.* **1981**, 85, 1137.
- [24] J.-F. Dufrêche, O. Bernard, P. Turq, *J. Chem. Phys.* **2002**, 116, 2085.
- [25] D. C. Douglass, H. L. Frisch, *J. Phys. Chem.* **1969**, 73, 3039.
- [26] Y. Ma, M. Doyle, T. F. Fuller, M. M. Doeff, L. C. de Jonghe, J. Newman, *J. Electrochem. Soc.* **1995**, 142, 1859.
- [27] M. A. Gebbie, A. M. Smith, H. A. Dobbs, A. A. Lee, G. G. Warr, X. Banquy, M. Valtiner, M. W. Rutland, J. N. Israelachvili, S. Perkin, R. Atkin, *Chem. Commun.* **2017**, 53, 1214.
- [28] K. R. Harris, *J. Phys. Chem. B* **2019**, 123, 7014.
- [29] M. Watanabe, *Electrochemistry* **2016**, 84, 642.
- [30] Y. Wang, W. Chen, Q. Zhao, G. Jin, Z. Xue, Y. Wang, T. Mu, *Phys. Chem. Chem. Phys.* **2020**, 22, 25760.
- [31] O. Nordness, J. F. Brennecke, *Chem. Rev.* **2020**, 120, 12873.
- [32] A. A. Lee, D. Vella, S. Perkin, A. Goriely, *J. Phys. Chem. Lett.* **2015**, 6, 159.
- [33] B. Roling, J. Kettner, V. Miß, *Energy Environ. Mater.* **2022**, 5, 6.
- [34] N. M. Vargas-Barbosa, B. Roling, *ChemElectroChem* **2020**, 7, 367.
- [35] B. Roling, C. Martiny, S. Brückner, *Phys. Rev. B* **2001**, 63, 214203.
- [36] C. Schröder, *J. Chem. Phys.* **2011**, 135, 24502.
- [37] V. Zeindlhofer, L. Zehetner, W. Paschinger, A. Bismarck, C. Schröder, *J. Mol. Liq.* **2019**, 288, 110993.
- [38] N. Bjerrum, *Kgl. Danske Videnskab Selskab* **1926**, 7, 9.
- [39] S. Zugmann, M. Fleischmann, M. Amereller, R. M. Gschwind, H. D. Wiemhöfer, H. J. Gores, *Electrochim. Acta* **2011**, 56, 3926.
- [40] M. Maiti, A. N. Krishnamoorthy, Y. Mabrouk, D. Diddens, A. Heuer, to be published.
- [41] Z. Li, R. Bouchal, T. Mendez-Morales, A.-L. Rollet, C. Rizzi, S. Le Vot, F. Favier, B. Rotenberg, O. Borodin, O. Fontaine, M. Salanne, *J. Phys. Chem. B* **2019**, 123, 10514.
- [42] D. Dong, D. Bedrov, *J. Phys. Chem. B* **2018**, 122, 9994.
- [43] S. Pfeifer, F. Ackermann, F. Sälzer, M. Schönhoff, B. Roling, *Phys. Chem. Chem. Phys.* **2021**, 23, 628.
- [44] K. Shigenobu, K. Dokko, M. Watanabe, K. Ueno, *Phys. Chem. Chem. Phys.* **2020**, 22, 15214.
- [45] K. Shigenobu, M. Shibata, K. Dokko, M. Watanabe, K. Fujii, K. Ueno, *Phys. Chem. Chem. Phys.* **2021**, 23, 2622.